

Hybrid method for simulating front propagation in reaction-diffusion systems

Esteban Moro*

Grupo Interdisciplinar de Sistemas Complejos (GISC) and Departamento de Matemáticas, Universidad Carlos III de Madrid,
Avenida de la Universidad 30, E-28911 Leganés, Spain

(Received 28 January 2004; published 2 June 2004)

We study the propagation of pulled fronts in the $A \leftrightarrow A+A$ microscopic reaction-diffusion process using Monte Carlo simulations. In the mean field approximation the process is described by the deterministic Fisher-Kolmogorov-Petrovsky-Piscounov equation. In particular, we concentrate on the corrections to the deterministic behavior due to the number of particles per correlated volume Ω . By means of a hybrid simulation scheme, we manage to reach large macroscopic values of Ω , which allows us to show the importance in the dynamics of microscopic pulled fronts of the interplay of microscopic fluctuations and their macroscopic relaxation.

DOI: 10.1103/PhysRevE.69.060101

PACS number(s): 05.40.-a, 68.35.Ct, 05.10.-a

When describing systems at much larger scales than the correlation length, internal fluctuations due to the intrinsic discreteness of the particles can be neglected, since they account for a correction typically only of the order of $\Omega^{-1/2}$, where Ω is the number of particles in a correlated volume. However, in some situations the dynamics of the system spans different scales, which gives rise to a strong dependence of its macroscopic features on the microscopic details of its constituents, even in the limit $\Omega \rightarrow \infty$. Relevant instances of this phenomena are the dynamic contact angle problem [1], evolution of a fracture tip [2], dendritic growth [3], and the flow of a gas through a microscopic channel [4]. In this paper we highlight and study another important example, namely, the effect of internal fluctuations in the macroscopic dynamics of pulled fronts [5,6]. Specifically, we consider the propagation of pulled fronts in reaction-diffusion microscopic problems, like the $A \leftrightarrow A+A$ scheme [7–9]. A continuum description of the system is possible in the reaction-limited regime where Ω is large enough so the reaction is well stirred within each correlated volume [7,9]. In this case, the density $\rho(x,t)$ of particles per correlated volume is described, in the limit $\Omega \rightarrow \infty$, by the Fisher-Kolmogorov-Petrovsky-Piscounov (FKPP) equation [10]

$$\frac{\partial \rho}{\partial t} = D \frac{\partial^2 \rho}{\partial x^2} + k_1 \rho - k_2 \rho^2. \quad (1)$$

This equation has traveling-wave solutions of the form $\rho = \rho(x-vt)$ which invade the unstable phase $\rho(\infty)=0$ from the stable phase $\rho(-\infty)=k_1/k_2$ and travel with velocity $v \geq v_0 = 2\sqrt{Dk_1}$. Of particular interest is the solution with velocity v_0 , since it is dynamically selected for a broad class of initial conditions. Moreover, v_0 is the linear spreading speed of infinitesimal perturbations around the unstable state. Thus, fronts with velocity v_0 are essentially “pulled along” by the growth and spreading of small perturbations in the leading edge $x \gg vt$ where $\rho \ll 1$. This sensitivity also causes the *ab-*

sence of a typical macroscopic length and time scale in which perturbations around the asymptotic solution with velocity v_0 are damped [5]. For example, the velocity of the front starting from a steep enough initial condition approaches the asymptotic value like a power law,

$$v(t) = v_0 - \frac{3}{2q_0 t} + \mathcal{O}(t^{-3/2}), \quad (2)$$

where $q_0 = v_0/2D$.

In particle models, however, the continuum description given by the FKPP equation breaks down at $\rho \approx 1/\Omega$ where internal fluctuations are important. Since pulled front dynamics are sensitive to infinitesimal events at $\rho \ll 1$, we expect macroscopic properties to depend strongly on Ω when $\Omega \rightarrow \infty$. For example, by neglecting microscopic fluctuations and mimicking the discreteness of particles by imposing an effective cutoff in the FKPP equation at $\rho = \Omega^{-1}$, Brunet and Derrida [11,12] obtained that the velocity is given by

$$v(\infty) \equiv v_\Omega = v_0 - \frac{v_0 \mathcal{K}_v}{\ln^2 \Omega} + \mathcal{O}(\ln^{-5/2} \Omega), \quad (3)$$

where \mathcal{K}_v is a constant. As expected the correction to the macroscopic velocity of the front is very strong: in a macroscopic volume of 10^{23} particles, it is still 0.3%. Combining Eqs. (2) and (3), we can easily infer that the typical time scale of microscopic pulled fronts is given by the condition $v(\tau_\Omega) \approx v_\Omega$, that is [13],

$$\tau_\Omega \sim \ln^2 \Omega. \quad (4)$$

Thus, pulled fronts in reaction-diffusion particle models do have a typical time scale, as opposed to those of the FKPP equation, although it is set by microscopic details and diverges in the limit $\Omega \rightarrow \infty$ [14].

Numerical confirmation of these predictions in general reaction-diffusion particle models is difficult, since the observation of the functional dependence in Eq. (3) requires typical simulations up to two orders of magnitude in $\ln \Omega$, which are not computationally feasible. However, for a particular model in which particles undergo nonlocal diffusion

*Electronic address: emoro@math.uc3m.es; http://gisc.uc3m.es/~moro

movements, Brunet and Derrida were able to perform simulations up to $\Omega \approx 10^{150}$ and check the prediction (3) with high accuracy [11,12]. Moreover, they also found that the front diffuses in time and that the diffusion coefficient behaves as [12]

$$D_\Omega \approx \frac{\mathcal{K}_D}{\ln^3 \Omega}, \quad (5)$$

where \mathcal{K}_D is a constant. While the velocity correction (3) can be easily understood in terms of an effective cutoff in the FKPP equation [11], and simulations for moderate numbers of particles ($\Omega \leq 10^{10}$) in reaction-diffusion particle models *seem to be compatible* with Eq. (3) [6,9,13,15], the functional dependence of D_Ω has been observed only in the non-local model of Brunet and Derrida. Although there is a heuristic argument for a specific model to get the $\ln^{-3} \Omega$ dependence [6], the situation clearly remains unsatisfactory, since there is only one empirical observation of Eq. (5). Thus, our purpose in this paper is to simulate the $A \leftrightarrow A+A$ model for very large number of particles in order to check both Eq. (3) and Eq. (5) and get some insight into the dynamics of pulled fronts in microscopic particle models.

The $A \leftrightarrow A+A$ model in one dimension consists of particles on a lattice with spacing Δx in which the number of particles at site i , $N_i(t)$, is unbounded (see [8]). Reaction events take place on site, while diffusion drives particles to nearest neighbor positions. Particles annihilate with rate σ , create another one with rate γ , and diffuse with rate D . In equilibrium, the average number of particles per site is $\Omega = \gamma/\sigma$, and when $\Omega \rightarrow \infty$ the system is described by Eq. (1) with $\rho(x,t) = N(x,t)/\Omega$ and $k_1 = k_2 = \gamma$. Early Monte Carlo (MC) simulations of this model [8] showed that indeed, when $\Omega \gg 1$, FKPP pulled fronts emerge. Specifically, it was found that both the velocity correction and the diffusion coefficient of the front decay like $\Omega^{-1/3}$ for $\Omega \leq 10^6$, a scaling which has been observed in other models for moderate values of Ω [15]. However, in order to observe the scalings (3) and (5) much larger numbers of particles are needed (typically $\Omega \gg 10^{10}$) which cannot be attained in standard MC simulations.

To reach larger numbers of particles in the $A \leftrightarrow A+A$ model, we note that, since the dynamics of pulled fronts are very sensitive to the dynamics of the system close to the unstable state $\rho \approx 0$, a correct description of the reaction-diffusion microscopic problem is needed only there, where fluctuations are important [12]. Away from the unstable state, i.e., when $\rho = \mathcal{O}(1)$, the number of particles is big enough so that fluctuations are negligible and the system can be safely described by macroscopic descriptions like Eq. (1). Thus we propose to split the dynamics of the microscopic model into two different descriptions: given a mesoscopic number of particles N^* with $\Omega \gg N^* \gg 1$, at any time step t we identify the position i^* as the smallest value of i for which $N_i(t) \leq N^*$. In the region in which fluctuations can be safely ignored, that is, when $i < i^*$, we update the number of particles using a numerical approximation of Eq. (1), while we use MC methods in the region $i \geq i^*$. To complete the algorithm, boundary conditions at $i = i^*$ should be given. Since only

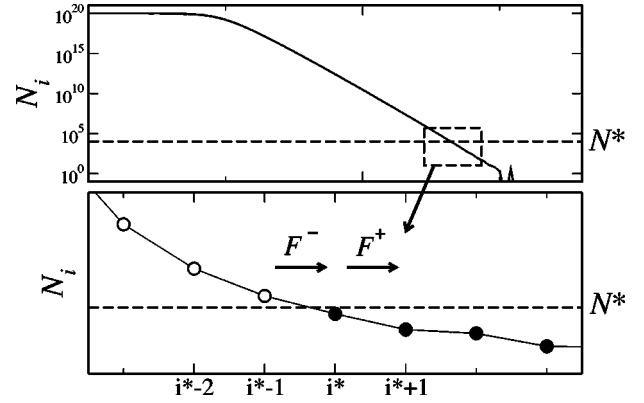


FIG. 1. Snapshot of the front profile for one realization of the hybrid method with $\Omega = 10^{20}$ (upper panel). Below: schematic view of the front $N_i(t)$ close to i^* . Open symbols are in the macroscopic region and full symbols in the microscopic region. For each lattice point i we define the flux of outgoing $F_i^+(t)$ and incoming $F_i^-(t)$ particles. In the figure only those for i^* are shown. Lines are guides to the eye.

diffusion couples the dynamics between different sites, we implement the boundary condition through the conservation of fluxes of particles through the boundary, similarly to other MC hybrid methods [16–18].

To this end, if we define at each site i the flux of incoming particles $F_i^-(t)$ and of outgoing particles $F_i^+(t)$ (see Fig. 1), the Euler approximation with time step Δt of Eq. (1) reads

$$\frac{N_i(t + \Delta t) - N_i(t)}{\Delta t} = \frac{F_i^-(t) - F_i^+(t)}{\Delta x} + \gamma N_i(t) - \sigma N_i^2(t) \quad (6)$$

with

$$F_i^-(t) = \frac{D}{\Delta x} [N_{i-1}(t) - N_i(t)],$$

$$F_i^+(t) = \frac{D}{\Delta x} [N_i(t) - N_{i+1}(t)]. \quad (7)$$

Obviously, conservation of the number of particles requires that $F_i^-(t) = F_{i-1}^+(t)$ and $F_i^+(t) = F_{i+1}^-(t)$. Thus, our algorithm evolves as follows. For a given mesoscopic time step $\Delta \tilde{t}$, we update the microscopic region ($i \geq i^*$) using a time continuous MC method [8] until the time of the simulation Δt exceeds $\Delta \tilde{t}$. Note that the typical time step in the MC simulation is given by $\delta t^{-1} \approx N^* [1 + \log(\Omega/N^*)]$ [19], which is smaller than $\Delta \tilde{t}$ in our simulations. Thus, several MC events take place until the MC simulation time Δt exceeds $\Delta \tilde{t}$, which makes the real Δt different for any time step. Any MC event in which a particle jumps into the macroscopic region ($i < i^*$) is recorded in the variable N^- , and the particle is removed from the MC simulation. We then update sites $i \leq i^* - 2$ using Eqs. (6) and (7). Finally, the number of particles at the boundary site $i^* - 1$ is updated using Eq. (6) but with $F_{i^*-1}^+$ calculated according to the MC recorded number of jumps, N^- . Specifically, we take $F_{i^*-1}^+ = (D/\Delta x) N_{i^*-1}(t) - N^- / (\Delta t \Delta x)$. Since we should get that $F_{i^*}^-(t) = F_{i^*-1}^+(t)$, we

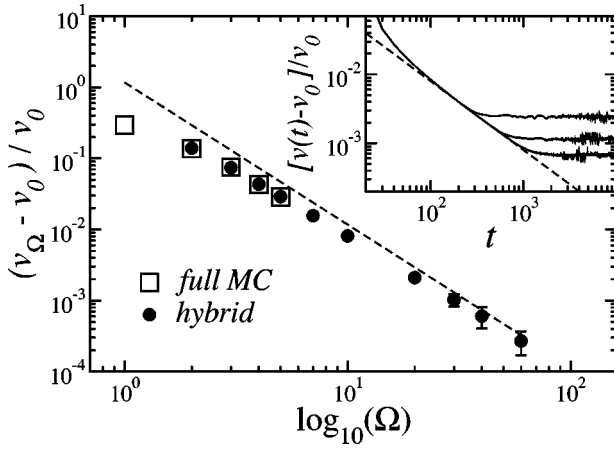


FIG. 2. Asymptotic velocity correction as a function of the logarithm of the number of particles Ω . Open symbols are results for the full MC simulation while full symbols are for the hybrid scheme. Dashed line corresponds to the scaling given by Eq. (3) with \mathcal{K}_v given by Eq. (9). Error bars are not shown when smaller than the symbol size. Inset: time evolution of the instantaneous velocity of the front (solid lines) with $\Omega = 10^{20}, 10^{30}$, and 10^{40} from top to bottom. Dashed line is the prediction given by Eq. (2).

update the number of particles at site i^* to satisfy this condition on average: $N_{i^*}(t + \Delta t) = N_{i^*}(t) + \Pi_{\Delta t} N_{i^*}(t) / \Delta x$ where Π_{λ} is a Poisson random number with mean λ . This completes a time step Δt in the algorithm.

The condition for a sharp interface between the macroscopic and the microscopic regions at i^* can be relaxed by introducing a buffer region [16,17]. Moreover, fluctuations can also be considered in the macroscopic region by adding an internal noise source to the FKPP equation [16,20]. However, for large enough N^* and small enough $\Delta \tilde{\tau}$, our results do not differ from those of these algorithm refinements. In our simulations we take $\Delta \tilde{\tau} = 10^{-4}$, $N^* = \min\{10^4, \Omega/2\}$, and $D = \gamma = \Delta x = 1$.

Results for this hybrid scheme are shown in Figs. 2 and 3 and compared with full MC simulations up to $\Omega = 10^5$. In each realization, the front position is defined by the place in the lattice where $\rho(x, t) = 1/2$. Both the correction to the velocity of the front (3) and the diffusion coefficient (5) agree, up to statistical fluctuations, with those of the full MC simulations, which supports the validity of our algorithm. Note that when $\Omega \rightarrow \infty$ our algorithm reduces to the Euler approximation of the FKPP equation. Thus, the velocity v_0 in (3) is given by the solutions of the equations [21]

$$\begin{aligned} v_0 e^{-q_0 v_0 \Delta \tilde{\tau}} &= -2 \sinh q_0, \\ e^{-q_0 v_0 \Delta \tilde{\tau}} &= 2 \Delta \tilde{\tau} [(\cosh q_0 - 1) - 1], \end{aligned} \quad (8)$$

and the velocity correction coefficient obtained using the efficient deterministic cutoff argument of [11] is given by

$$\mathcal{K}_v = \pi^2 q_0 (e^{v_0 q_0 \Delta \tilde{\tau}} \cosh q_0 - v_0^2 \Delta \tilde{\tau} / 2). \quad (9)$$

In the limit $\Omega \rightarrow \infty$ we observe in Fig. 2 that our results tend to the scaling (3) together with the solutions (8) and (9).

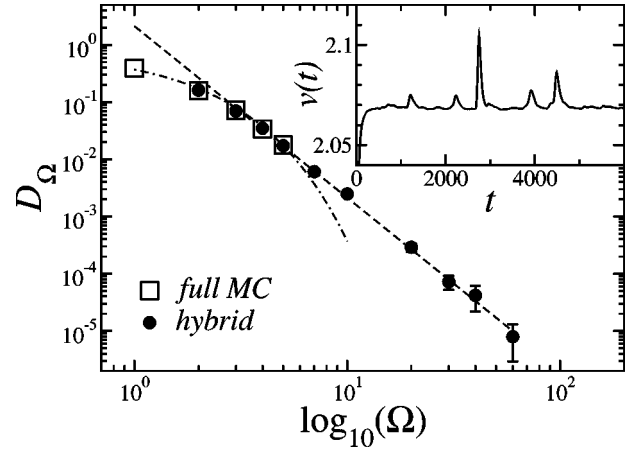


FIG. 3. Diffusion coefficient of the front D_f as a function of the logarithm of the number of particles Ω . Symbols are as in Fig. 2. Dashed line is a fit of the last points to the scaling form (5) with $\mathcal{K}_D = 26.5$. Dot-dashed line is the scaling $D_f \sim \Omega^{-0.32}$ of [8]. Error bars are not shown when smaller than the symbol size. Inset: Velocity as a function of time for one realization of the algorithm with $\Omega = 10^{20}$.

However, a strong deviation of our results for the predicted scaling (3) even for large values of Ω is observed, a fact that also was present in the Brunet and Derrida model [12]. Asymptotic convergence of microscopic pulled fronts in the $A \leftrightarrow A + A$ toward the solution of the FKPP equation is also observed in the inset of Fig. 2, in which we plot the time dependence of the velocity for different values of Ω . As expected, in our simulations the velocity decays accurately like Eq. (2) until it saturates to a constant value given by Eq. (3).

Regarding the diffusion coefficient, our results for the $A \leftrightarrow A + A$ confirm the scaling (5) found in [12]. Note that the results for small values of Ω agree with the scaling $D_\Omega \sim \Omega^{-1/3}$ found in the initial studies of the $A \leftrightarrow A + A$ model [8]. To understand the origin of the functional dependence of the diffusion coefficient, we show in the inset of Fig. 3 a typical realization of the instantaneous velocity of the front as a function of time. As we can see, long-lived fluctuations occur at the front, whose origin is in the large relaxation time of microscopic pulled front dynamics, $\tau_\Omega \sim \ln^2 \Omega$. In order to check this, we have measured the time correlation of the instantaneous velocity of the front for different values of Ω :

$$C_v(t) \equiv \langle [v(s+t) - v_\Omega][v(s) - v_\Omega] \rangle. \quad (10)$$

Our data (see Fig. 4) indicate that the velocity correlation scales like

$$C_v(t) \sim \frac{1}{\ln^5 \Omega} G\left(\frac{t}{\ln^2 \Omega}\right), \quad (11)$$

where $G(x)$ is a scaling function. As expected, the relaxation time of velocity fluctuations is given by τ_Ω and, in particular, Eq. (11) is consistent with the scaling of D_Ω given by Eq. (5) using the Kubo formula

$$D_\Omega \sim \lim_{t \rightarrow \infty} \int_0^t C_v(t') dt' \sim \frac{1}{\ln^3 \Omega}. \quad (12)$$

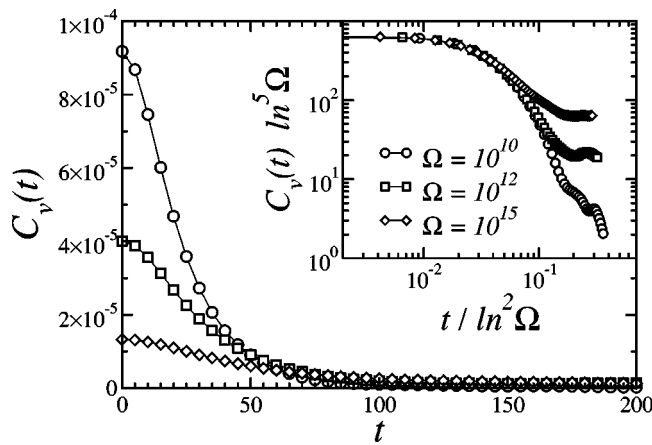


FIG. 4. Velocity time correlation as a function of time for different values of the number of particles Ω . Inset shows the scaling given by Eq. (11).

The observed scaling (11) gives us some insight into the effect of internal fluctuations in microscopic pulled fronts: at small densities, fluctuations in the number of particles $N_i(t)$ become important (for example, note in Fig. 1 the presence of particles well ahead of the tip of the front). Equation (11) suggests that those fluctuations have a strength proportional to $1/\ln^5 \Omega$. In the existence of a typical macroscopic scale, those fluctuations would be damped almost instantaneously and the diffusion coefficient would have been proportional to $1/\ln^5 \Omega$. In fact, a similar result is obtained analytically for the coarse-grained continuous model (the stochastic FKPP

equation [20]) of the $A \leftrightarrow A+A$ model when standard perturbation techniques (which rely on the existence of a macroscopic time scale) are used [6]. However, microscopic pulled fronts do not have this macroscopic time scale, and fluctuations are accommodated by the dynamics on a much larger time scale τ_Ω . The interplay between the microscopic fluctuations of strength $\ln^{-5} \Omega$ and the time scale of order $\ln^2 \Omega$ in which they relax is what produces the dependence on $\ln \Omega$ observed in the diffusion coefficient.

In summary, we have presented a hybrid method for studying the dynamics of fronts in particle reaction-diffusion problems. This hybrid scheme allows us to investigate the asymptotic convergence of those microscopic models to the macroscopic description given by the FKPP equation (1). In particular, we reproduced the scaling of the velocity correction with the number of particles given by Eq. (3), observed in [11], and inferred in other works. More interestingly, we confirmed the proposed scaling for the diffusion coefficient (5) and showed that its origin is in the interplay of the typical relaxation time of microscopic pulled fronts and the strength of the microscopic fluctuations at small densities.

We would like to thank R. Cuerno, C. R. Doering, A. Sánchez, and P. Smereka for comments and discussions and the MCTP at University of Michigan and the DEAS at Harvard University for their hospitality during the progress of this work. This work has been supported by grants from the Ministerio de Ciencia y Tecnología and Comunidad de Madrid (Spain).

-
- [1] J. Koplik and J. R. Banavar, *Annu. Rev. Fluid Mech.* **27**, 257 (1995).
- [2] F. F. Abraham, J. Q. Broughton, N. Bernstein, and E. Kaxiras, *Comput. Phys.* **12**, 538 (1998).
- [3] M. Plapp and A. Karma, *Phys. Rev. Lett.* **84**, 1740 (2000).
- [4] F. Alexander, A. L. Garcia, and B. J. Alder, *Phys. Fluids* **6**, 3854 (1994); A. L. Garcia, J. B. Bell, W. Y. Crutchfield, and B. J. Alder, *J. Comput. Phys.* **154**, 134 (1999).
- [5] W. van Saarloos, *Phys. Rep.* **386**, 29 (2003); U. Ebert and W. van Saarloos, *Physica D* **146**, 1 (2000).
- [6] D. Panja, e-print cond-mat/0307363; *Phys. Rev. E* **68**, 065202 (2003).
- [7] D. ben-Avraham and S. Havlin, *Diffusion and Reactions in Fractals and Disordered Systems* (Cambridge University Press, Cambridge, England, 2000).
- [8] H. P. Breuer, W. Huber, and F. Petruccione, *Physica D* **73**, 259 (1993); *Europhys. Lett.* **30**, 69 (1995).
- [9] E. Moro, *Phys. Rev. Lett.* **87**, 238303 (2001); *Phys. Rev. E* **68**, 025102 (2003).
- [10] R. A. Fisher, *Ann. Eugenics* **7**, 355 (1936); A. Kolmogorov, I. Petrovsky, and N. Piscounov, *Mosc. Univ. Bull. Math. A* **1**, 1 (1937).
- [11] E. Brunet and B. Derrida, *Phys. Rev. E* **56**, 2597 (1997); *Comput. Phys. Commun.* **122**, 376 (1999).
- [12] E. Brunet and B. Derrida, *J. Stat. Phys.* **103**, 269 (2001).
- [13] D. A. Kessler, Z. Ner, and L. M. Sander, *Phys. Rev. E* **58**, 107 (1998).
- [14] Strictly speaking, only fronts with $\tau_\Omega \rightarrow \infty$ are pulled, while for finite and large τ_Ω they become weakly pushed; see [5].
- [15] A. Lemarchand and B. Nowakowski, *J. Chem. Phys.* **111**, 6190 (1999); A. Lemarchand, *J. Stat. Phys.* **101**, 579 (2000).
- [16] F. J. Alexander, A. L. García, and D. M. Tartakovsky, *J. Comput. Phys.* **182**, 47 (2002).
- [17] E. G. Flekkøy, J. Feder, and G. Wagner, *Europhys. Lett.* **52**, 271 (2000); *Phys. Rev. E* **64**, 066302 (2001).
- [18] T. P. Schulze, P. Smereka, and W. E, *J. Comput. Phys.* **189**, 197 (2003).
- [19] The typical time step in a MC simulation is $\delta t \approx 1/M$, where M is the total number of particles. Assuming that the front has the shape $\rho(\xi, t) = \xi e^{-\xi}$ we can approximate $\delta t^{-1} \approx M = \Omega \int_{x^*}^{\infty} \rho(\xi, t) d\xi = N^* [1 + \log(\Omega/N^*)]$.
- [20] C. R. Doering, C. Mueller, and P. Smereka, *Physica A* **325**, 243 (2003).
- [21] L. Pechenik and H. Levine, *Phys. Rev. E* **59**, 3893 (1999).